

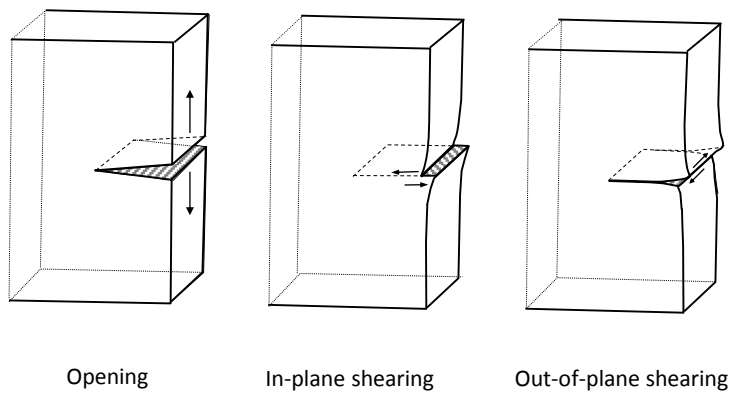


G. Hénaff

1



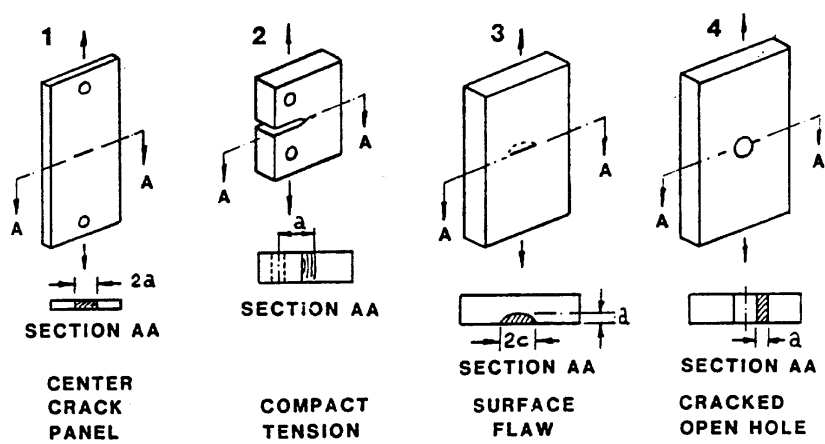
# Opening modes



G. Hénaff – 2016

3

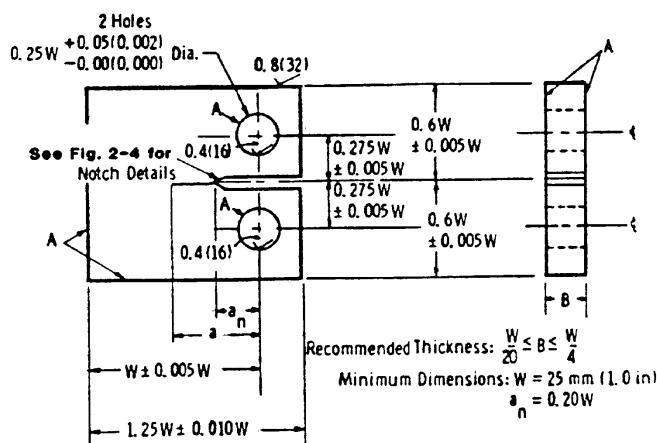
# Standard specimens



G. Hénaff – 2016

4

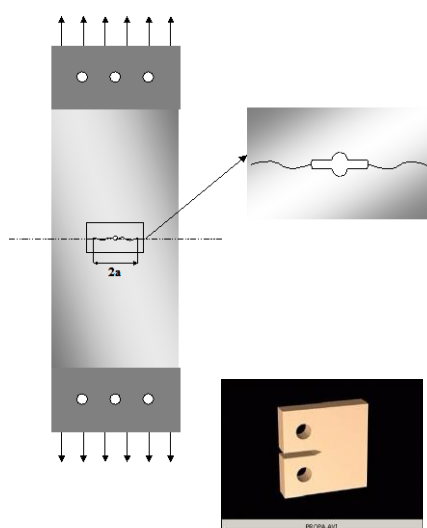
## Compact tension specimen



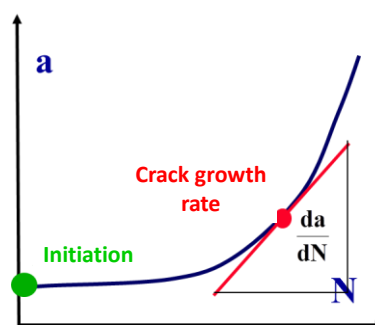
G. Hénaff – 2016

5

## Fatigue crack propagation test



- Pre-cracked specimens
- Crack length monitoring of the crack length as a function of the number of applied cycles (optical, compliance, potential drop)



6

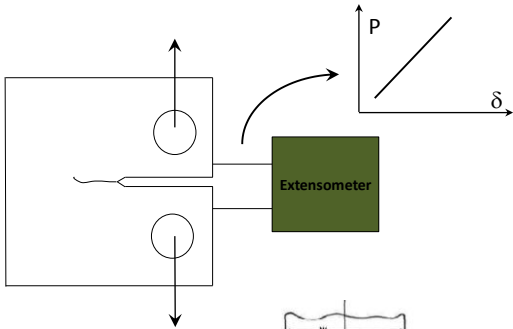
G. Hénaff – 2016

# Crack length monitoring

- Optical method (direct)

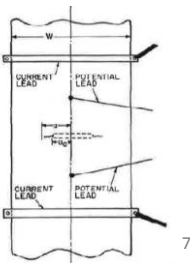


- Variation of Compliance



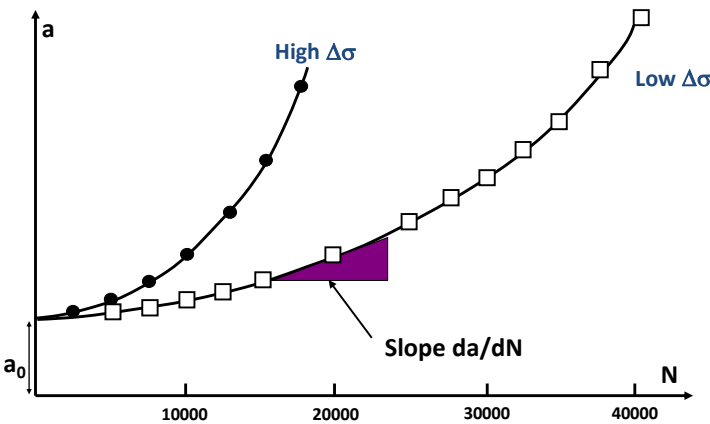
- Potential drop (requires a calibration)

$$\frac{V(a)}{V(a_0)} = \frac{\cosh^{-1}\left(\frac{\cosh \pi y / 2W}{\cosh \pi x / 2W}\right)}{\cosh^{-1}\left(\frac{\cosh \pi y / 2W}{\cosh \pi x_0 / 2W}\right)}$$



G. Hénaff – 2016

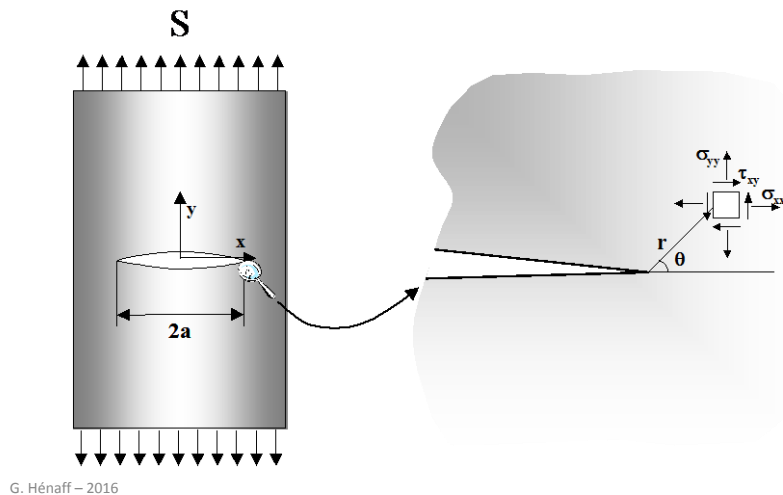
# Propagation curves



G. Hénaff – 2016

## Use of LEFM

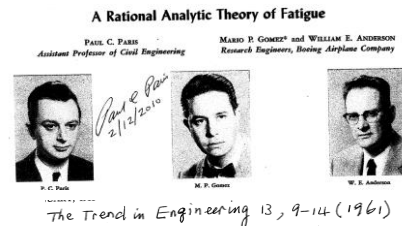
Static or monotonic loading: the stress intensity factor accounts for the stress/strain field at the crack tip



9

## Use of LEFM

Idea: consider the *stress intensity factor range*  $\Delta K$  as the *driving force* for crack growth under cyclic loading



$$\begin{aligned}\Delta K &= \alpha \times \Delta \sigma \times \sqrt{\pi a} \\ &= \alpha \times (\sigma_{\max} - \sigma_{\min}) \times \sqrt{\pi a} \\ &= K_{\max} - K_{\min}\end{aligned}$$

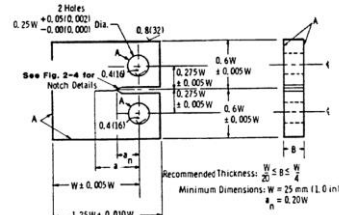


NB: even when  $\Delta \sigma$  is kept constant,  $\Delta K$  increases during crack growth

G. Hénaff – 2016

10

# Stress intensity factor



## COMPACT TENSION SPECIMEN

$$\Delta K = \frac{\Delta P}{B\sqrt{W}} \frac{(2+\alpha)}{(1-\alpha)^{3/2}} \left[ 0.886 + 4.64\alpha - 13.32\alpha^2 + 14.72\alpha^3 - 5.6\alpha^4 \right]$$

$$\alpha = a/W$$

WHERE  $\Delta P = P_{\max} - P_{\min}$  FOR  $R > 0$

$\Delta P = P_{\max}$  FOR  $R \leq 0$

THIS EXPRESSION IS VALID FOR  $a/W \geq 0.2$

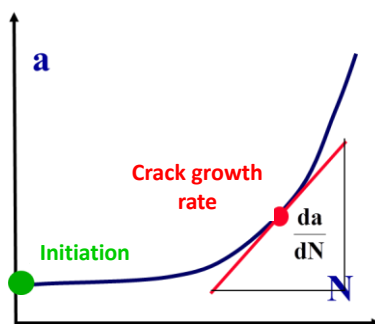
## CENTER CRACKED PANEL SPECIMEN

$$\Delta K = \frac{\Delta P}{B\sqrt{2W}} \sqrt{\frac{\pi\alpha}{2}} \sec \frac{\pi\alpha}{2} \quad \text{WHERE } \alpha = 2a/W$$

THIS EXPRESSION IS VALID FOR  $2a/W < 0.95$

11

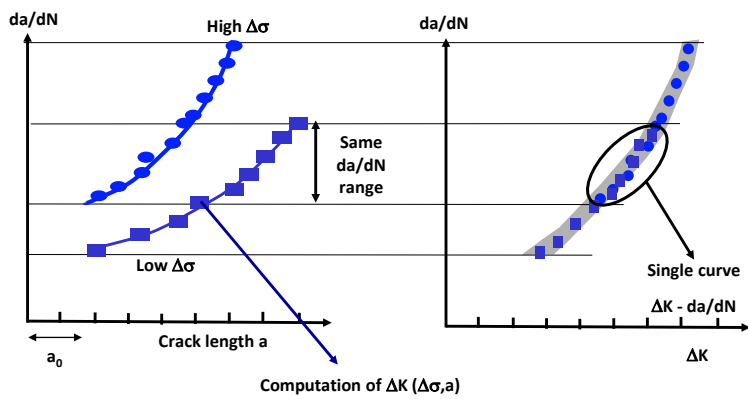
# LEFM concepts



Depends on specimen geometry, initial crack size, applied stress range, ...

Principle of similarity: a given value of  $\Delta K$  (for a wide variety of  $\sigma$  and  $a$  values) induces the same cyclic stress/strain field at the crack tip, therefore the same damage and as a consequence the same crack growth rate

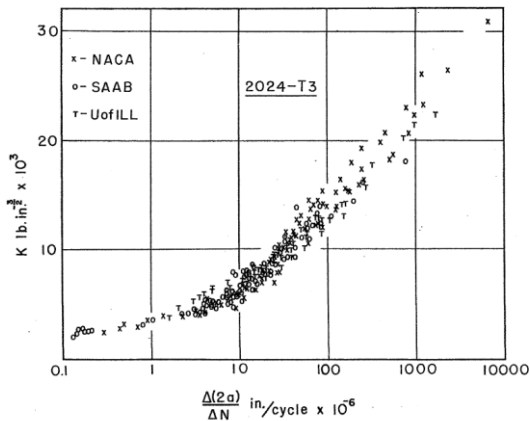
# Principle of similarity



G. Hénaff – 2016

13

# Paris correlation



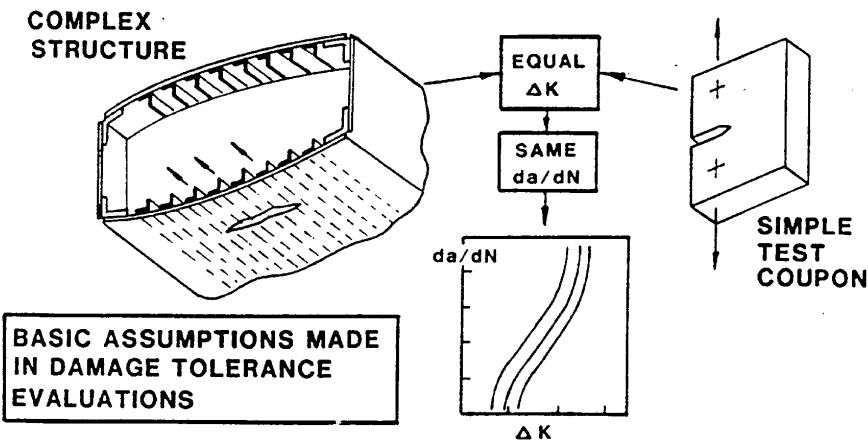
**Conclusion**

On the basis of the experimental data given, it is evident that rates of crack growth—for example, those in 2024-T3 and 7075-T6 skins of aircraft structure—may be computed by the theory presented over a wide range of nominal stress levels and crack sizes. The ramifications of such broad correlation imply an analytic theory of fatigue based on a concept of growth from initial imperfections through which structural life may be predicted.

G. Hénaff – 2016

14

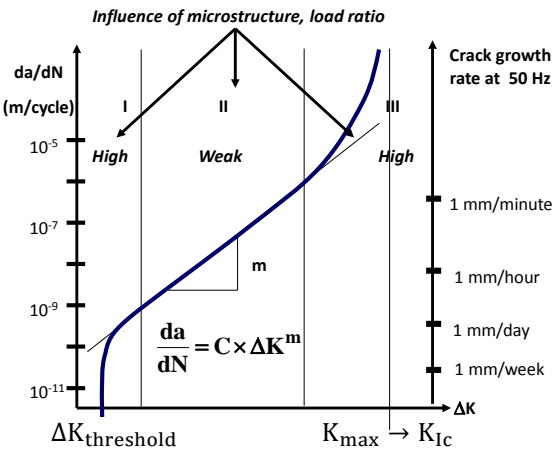
# Transposability of laboratory data to structures



G. Hénaff – 2016

15

## da/dN- $\Delta K$ curve



G. Hénaff – 2016

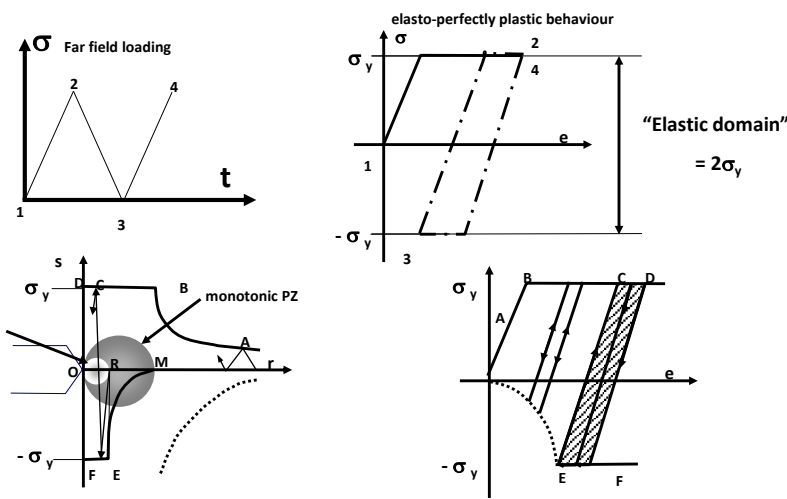
16



# Mechanisms

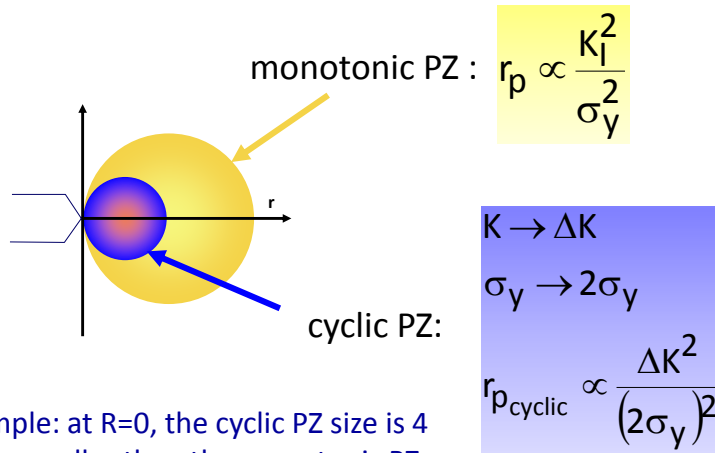
G. Hénaff – 2016

## Cyclic deformation at the crack tip



G. Hénaff – 2016

## Cyclic plastic zone size



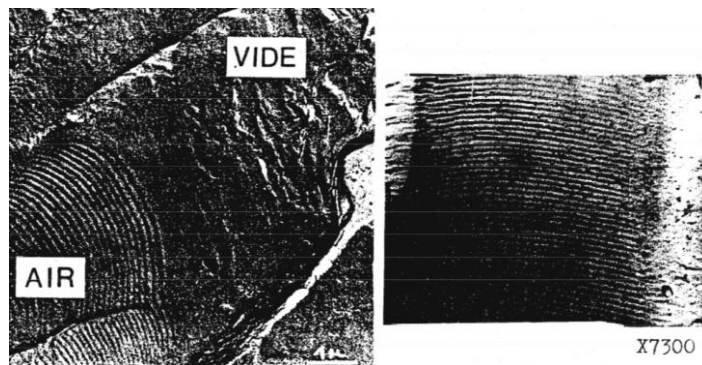
Example: at  $R=0$ , the cyclic PZ size is 4 times smaller than the monotonic PZ size.

G. Hénaff – 2016

19

## Propagation mechanisms: fatigue striations

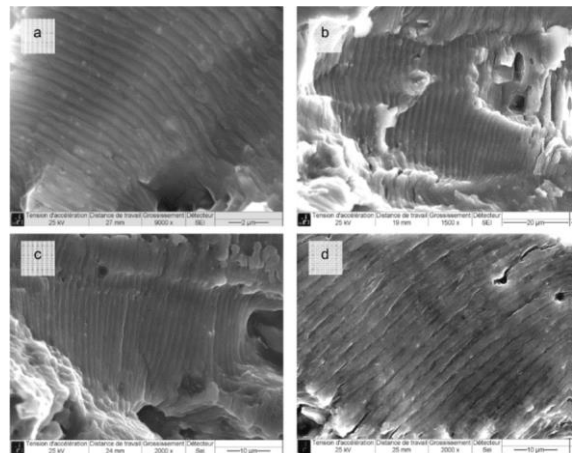
- Periodic markings on fracture surfaces;
- Intermediate crack growth rate range ( $5 \times 10^{-8}$  -  $10^{-5}$  m/cycle);
- Clearly defined in Aluminum alloys, much less in high strength alloys;
- No striation in inert environment.



G. Hénaff – 2016

20

# Propagation mechanisms: fatigue striations

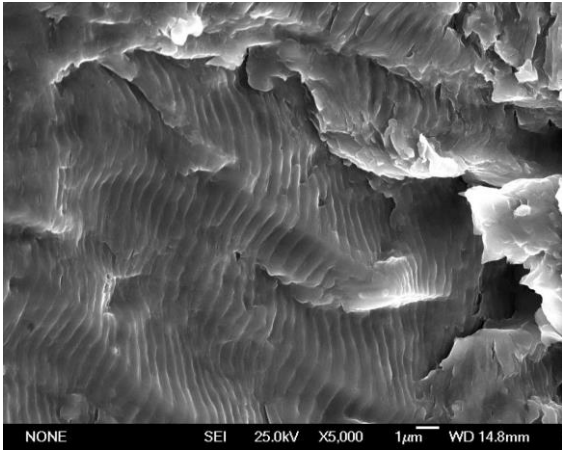


Striations after fatigue at  $R=0.1$  in a 2024 T351 alloy from the teardown of a A320 MSN004 wing: tip, maximum stress 400 MPa (a) and 300 MPa (b); engine area maximum stress 275 MPa (c) et 300 MPa (d) (Thèse F. Billy, ENSMA)

G. Hénaff – 2016

21

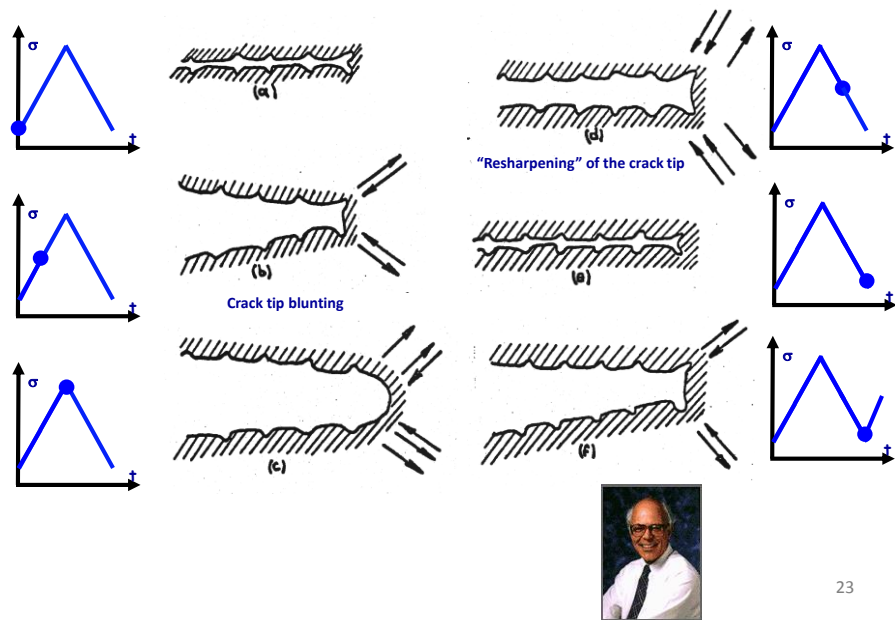
## Mécanismes de Propagation : Stries de Fatigue



Striations in a precipitation-hardened martensitic stainless steel used in aerostructures (thèse L. Dimithe-Aboumou, ENSMA)

22

# Striation formation: Laird mechanism



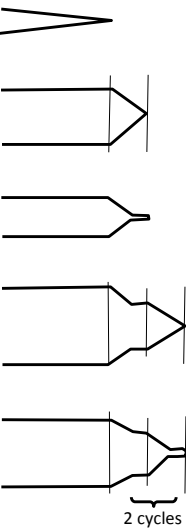
# Striation formation: Pelloux mechanism



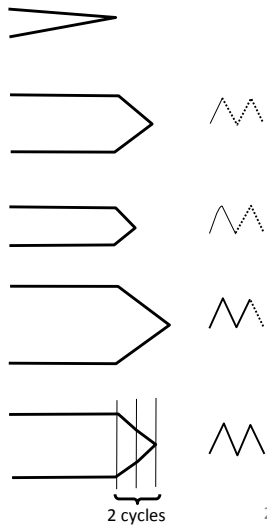
Dr. Regis Pelloux  
1931 - 2015

→ Accounts for  
the absence of  
striation in  
vacuum

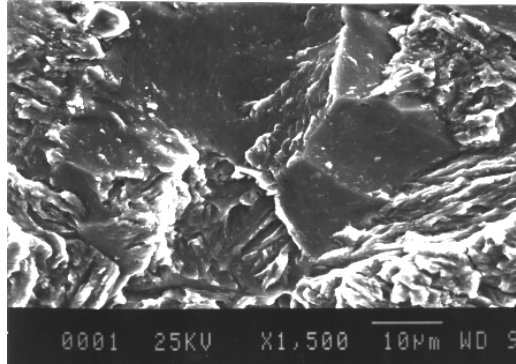
Irreversible slip  
(oxidation)



Reversible slip  
(inert)



## Propagation mechanisms in the near-threshold region



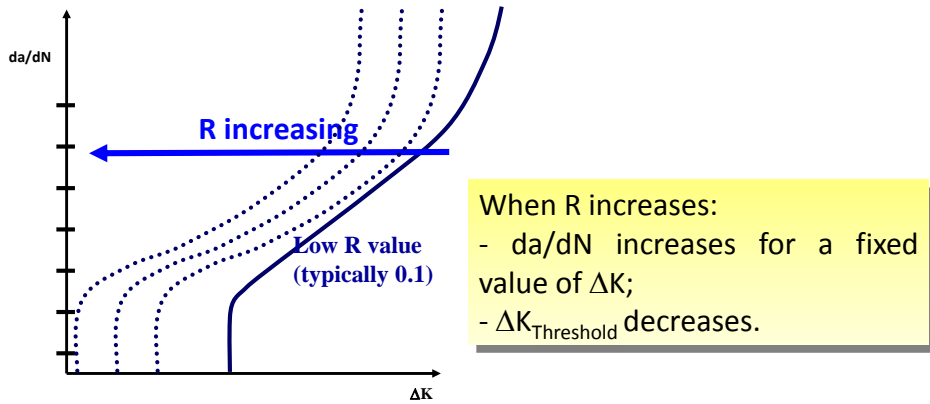
More brittle aspect of the fracture surfaces (cleavage-like fracture, intergranular decohesions,....)

G. Hénaff – 2016

25

## Factors of influence

## Influence of load ratio

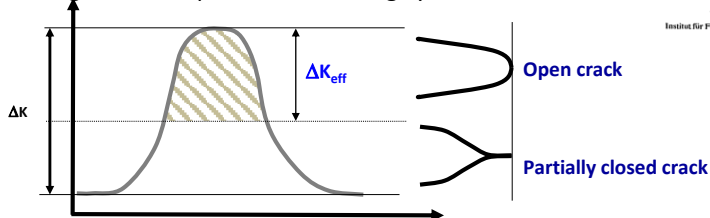


G. Hénaff – 2016

27

## Crack closure

Experimental evidence that a fatigue crack, even when loaded in tension ( $R > 0$ ) can be partially closed during the lower part of the loading cycle.



Hyp : a crack can propagate only when it is fully open  $\Rightarrow da/dN$  fonction of  $\Delta K_{\text{eff}}$

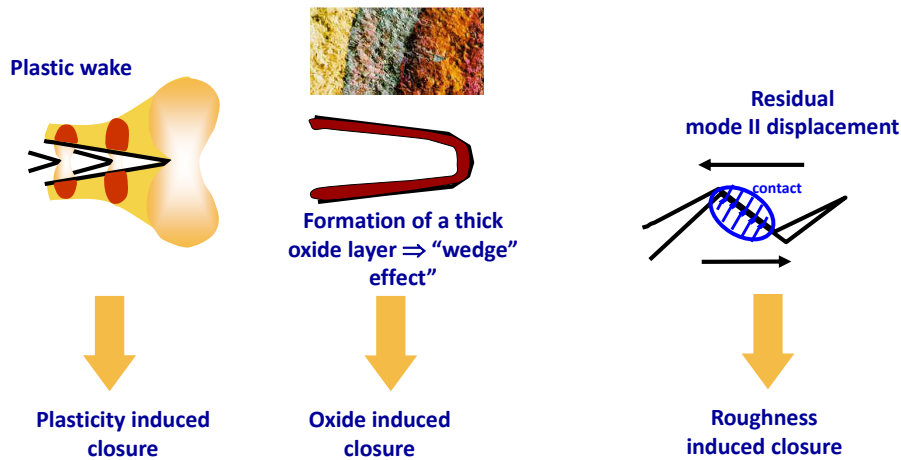
Elber (1970):  $\Delta K_{\text{eff}} = U \times \Delta K$

For the 2024 T351 alloy in Paris regime:  $U = a + b \times R$

G. Hénaff – 2016

28

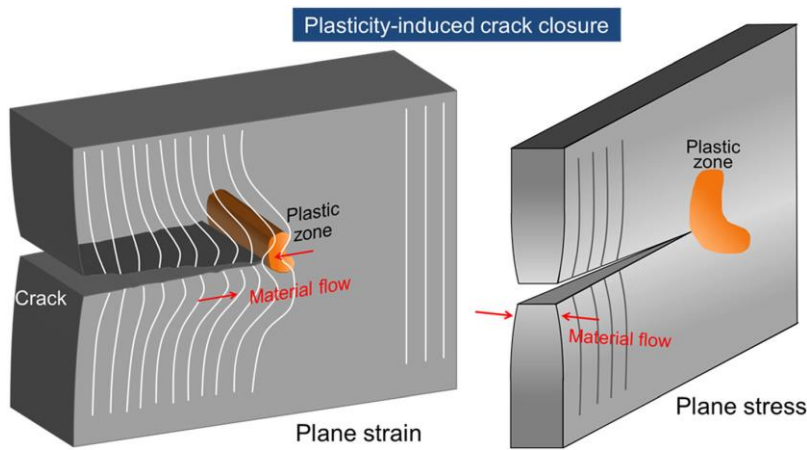
# Crack closure sources



G. Hénaff – 2016

29

## Plasticity-Induced Closure

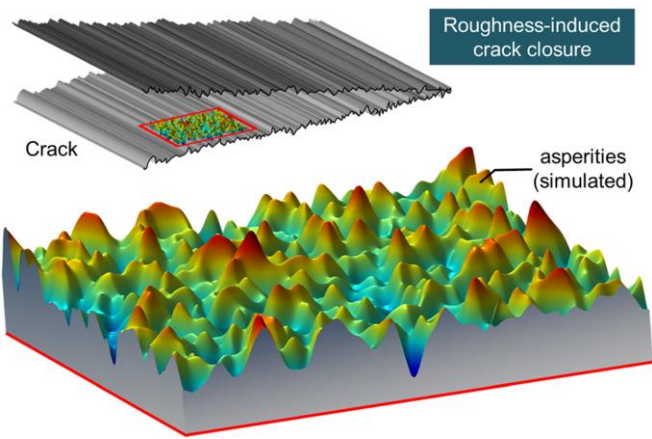


The material flow from the bulk that accumulates on the crack flanks, thereby giving rise to the premature contact as noted by Sun and Sehitoglu

G. Hénaff – 2016

30

# Roughness-Induced Closure

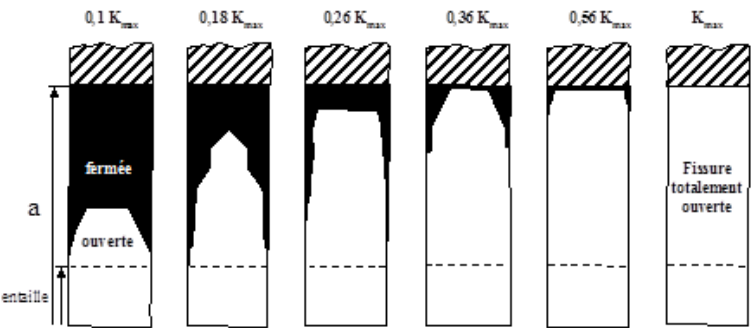


Garcia and Sehitoglu modelled roughness-induced crack closure as a contact problem with random distribution of surface asperities.

G. Hénaff – 2016

31

# Opening kinematics

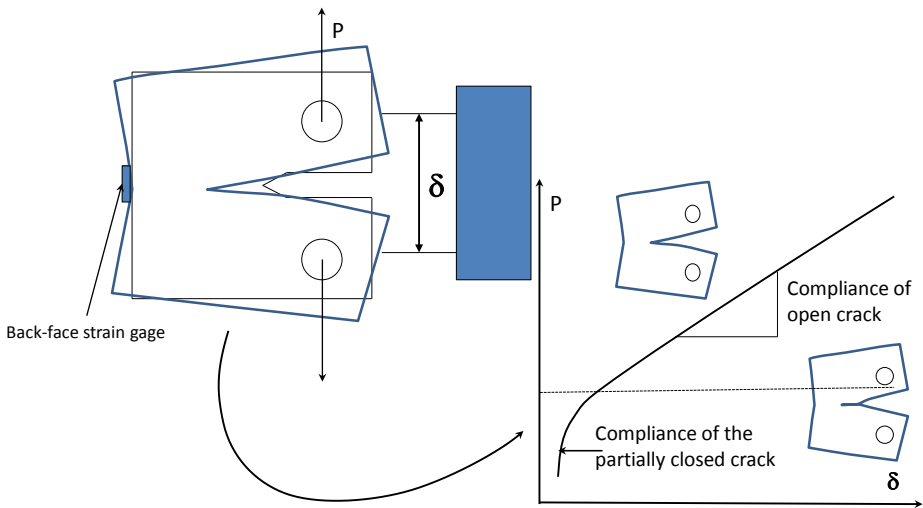


FEM Simulation of the crack opening in a CCT specimen (after Chermahini et al. 1988 ).

32



Experimental measurement of the crack opening load

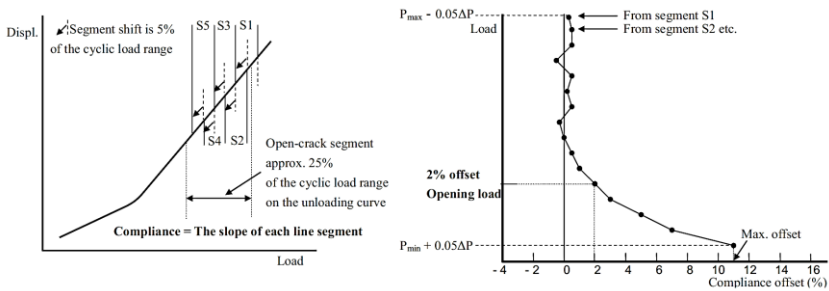


G. Hénaff – 2016

33

Experimental measurement of the crack opening load

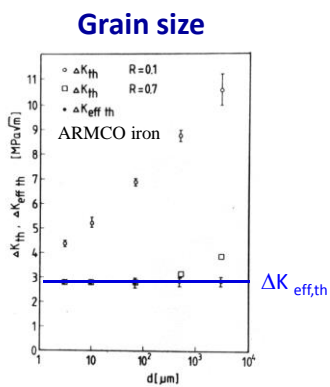
$$\text{Compliance offset}(\%) = \frac{[(\text{open-crack compliance}) - (\text{compliance})]}{(\text{open-crack compliance})} \times 100$$



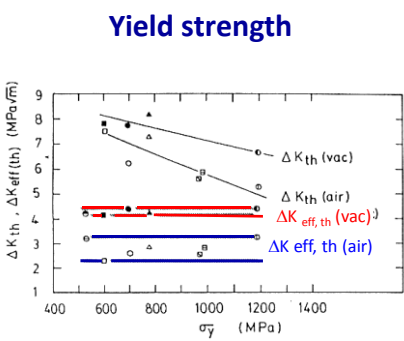
G. Hénaff – 2016

34

# Influence of metallurgical parameters



The coarser the grain, the higher the threshold  $\leftrightarrow$  crack closure effect

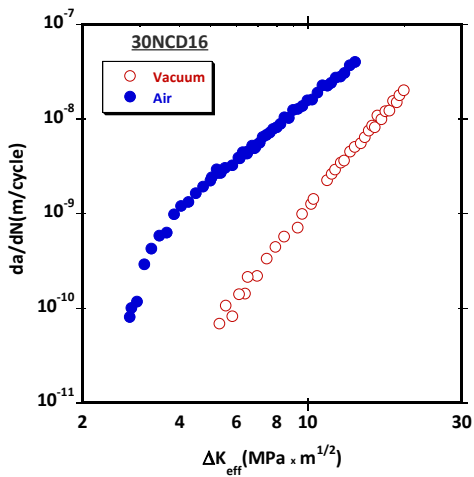


The higher the yield strength, the lower the threshold  $\leftrightarrow$  crack closure effect

G. Hénaff – 2016

35

# Influence of environment

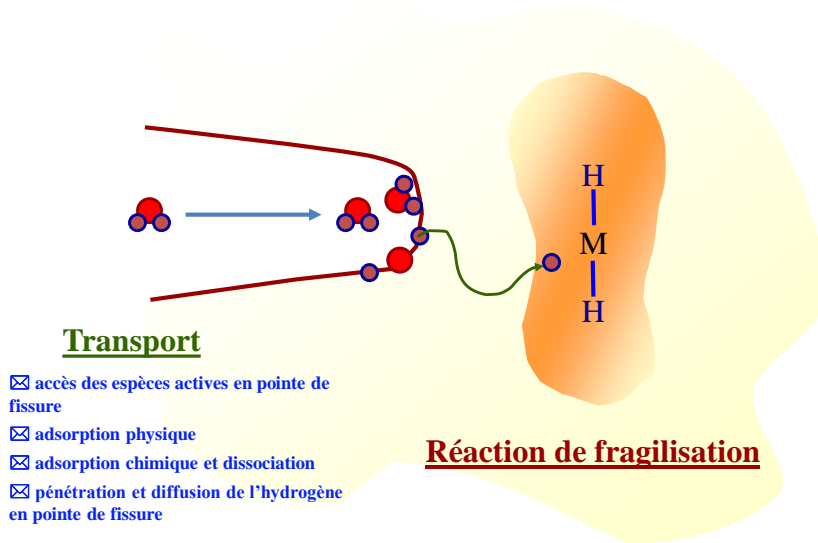


A moist environment induces a loss of resistance

G. Hénaff – 2016

36

## Propagation assistée par l'hydrogène



37

## Fatigue Crack Propagation Laws

Empirical Laws:

$$\frac{da}{dN} = C \times \Delta K^m$$

Paris

$$\frac{da}{dN} = \frac{C \times \Delta K^m}{((1-R)K_c - \Delta K)}$$

Forman

Theoretical approaches:

$$\frac{da}{dN} = A \times \frac{\Delta K^4}{\mu \sigma_0^2 U}$$

Cumulative  
damage at the  
crack tip

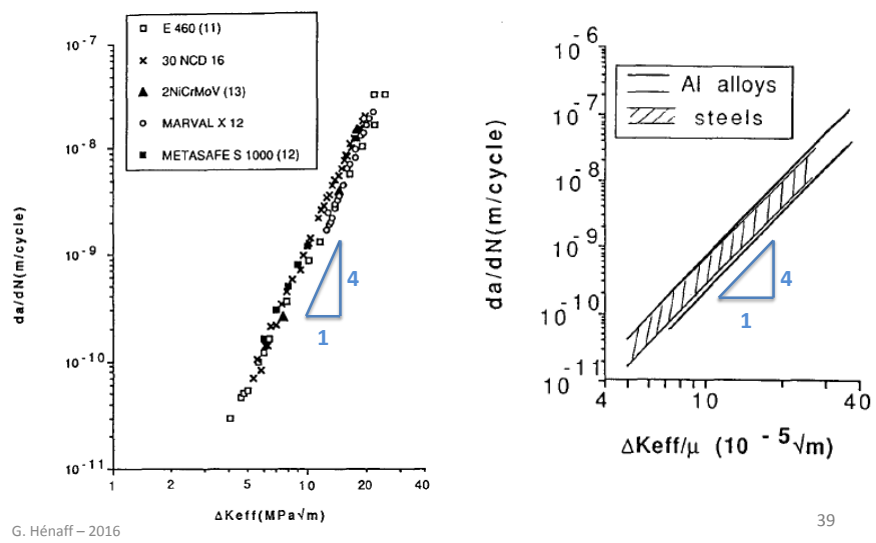
$$\frac{da}{dN} = A \times \frac{\Delta K^4}{\varepsilon_f E^2 \sigma_y^2 \rho}$$

Manson-Coffin at the  
crack tip (McClintock,  
Antolovitch,...)

$$\frac{da}{dN} = \frac{1}{2} \text{CTOD} = \frac{\Delta K^2}{2E\sigma_y}$$

CTOD (Pelloux)

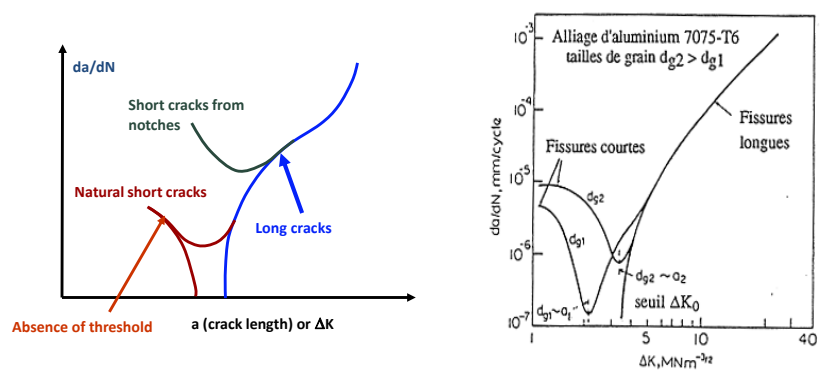
# Intrinsic fatigue crack growth (inert, $\Delta K_{eff}$ )



39

# Short cracks

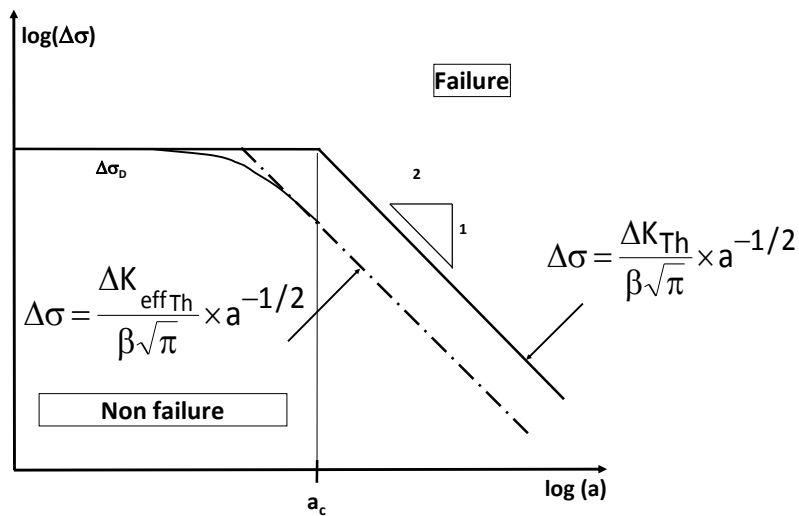
Def : cracks for which at least one dimension is small with respect to other dimensions (geometry, grain size,...)



G. Hénaff – 2016

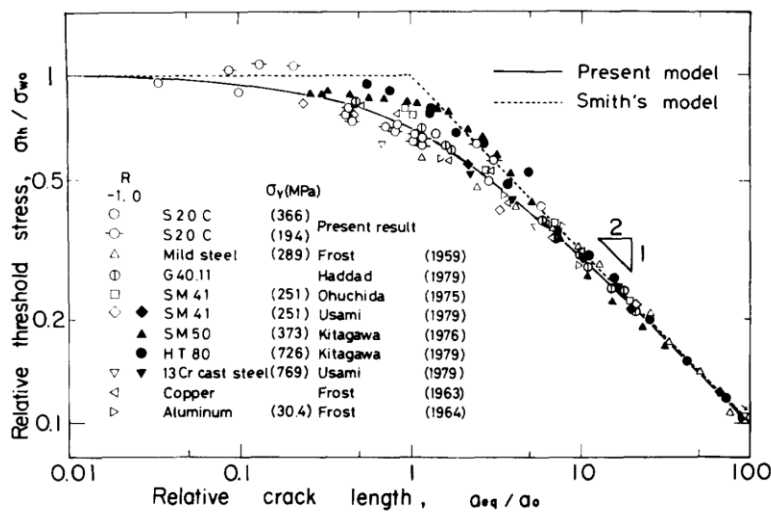
40

# Kitagawa diagram



G. Hénaff – 2016 41

# Kitagawa Diagram



G. Hénaff – 2016 42